A Guideline for Humanoid Leg Design with Oblique Axes for Bipedal Locomotion

Konrad Fründ, Anton Leonhard Shu, Florian Christoph Loeffl, and Christian Ott

***Abstract*— The kinematics of humanoid robots are strongly inspired by the human archetype. A close analysis of the kinematics of the human musculoskeletal system reveals that the human joint axes are oriented within certain inclinations. This is in contrast to the most popular humanoid design with a configuration based on perpendicular joint axes. This paper reviews the oblique joint axes of the mainly involved joints for locomotion of the human musculoskeletal system. We elaborate on how the oblique axes affect the performance of walking and running. The mechanisms are put into perspective for the locomotion types of walking and running. In particular, walking robots can highly benefit from using oblique joint axes. For running, the primary goal is to align the axis of motion to the mainly active sagittal plane. The results of this analysis can serve as a guideline for the kinematic design of a humanoid robot and a prior for optimization-based approaches.**

I. Introduction

The field of bipedal robotic locomotion is divided into the two main fields of walking and running. While there exist many walking robots with an e.g. inverted pendulum or rimless wheel locomotion template [1], [2], there are fewer humanoids which are capable of running. The widely used spring-mass or spring-loaded inverted pendulum (SLIP) templates of running require different kinematic solutions with a shift of thinking about bipedal robotic locomotion and especially about impacts, stability, and efficiency [3]–[6]. To achieve a feasible running performance, the kinematic is a valid starting point to optimize current design approaches.

The robot kinematic is a key component in the development of a humanoid robot. This paper introduces the human kinematic of the locomotion unit, explains promising mechanisms, and derives basic concepts for its application in humanoid robots. The human kinematic is used as an example, as it has been optimized for more than two million years of evolution for the daily living locomotion tasks of i.a. walking and running [7], [8]. The mechanisms of the human locomotion system are used to develop concepts that reduce the requirements of the actuation system of a humanoid robot.

The literature on mechanisms and functions that the human body has developed through the process of evolution is broad [7], [8]. Many are focused on skeletal differences between ancient types of homo and the homo sapiens. However, less attention is paid to the obliquity of the human-developed lower leg joint axes and the effect they have on the human motion [9]. Besides the literature about oblique foot joints, there is a gap which needs to be filled, of applying obliquities to the standard perpendicular leg axis to decrease the mechanical joint requirements and increase the robot efficiency. Fig. 1 shows the oblique axis of the knee and subtalar joint in the stance phase of walking. The most representative example is the knee joint, in which oblique axis can comprise three possible mechanisms: a passively stable stance phase, decreased actuator torques, and reduced constraint torques.

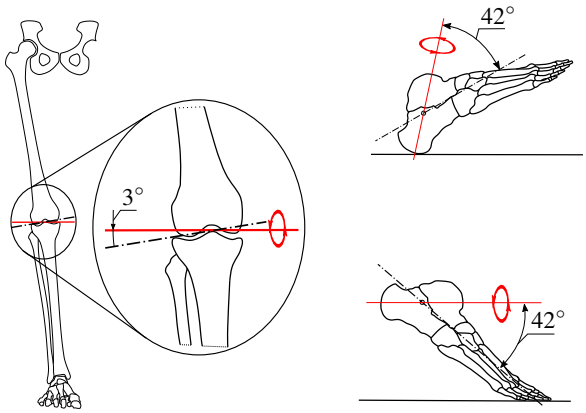

Fig. 1: The oblique knee axis at a narrow walking step-width and the subtalar joint axes at heel-strike and pre-swing phase. The oblique axes are shown in solid-red, the perpendicular axis as a dashed-dotted line.

In the field of humanoid robots, the author in [10] examined the effect of the human oblique joint axes on reproducing human kinematics. Other researchers, such as [11]–[13] applied these ideas to the robot development. Their applications include an oblique waist that can resolve singularities and increase reaching distance, as well as feet that can adapt to uneven terrain. Additionally, robots such as ARMAR IV, and LOLA are using oblique hip axis, which increase its maximum peak power in the movement direction [14], [15]. Biomimicing robots like Kengoroo might also use an oblique knee axis, however the topic was not being specifically addressed in their paper [16]. The topic of oblique axes is more present in the field of lower limb prosthetics to restore a symmetrical, and less obstructive gait in patients [17]. With this knowledge we want to elaborate chances and risks of applying oblique axis to a humanoid robot.

The major joints involved in walking and running are

This project has received funding from the European Research Council (ERC) under the European Union's Horizon 2020 research and innovation programme (grant agreement No. 819358).

Konrad Fründ, Anton Shu, and Florian Loeffl are with the Institute of Robotics and Mechatronics, German Aerospace Center (DLR), 82234 Wessling, Germany {konrad.fruend, anton.shu, florian.loeffl}@dlr.de

Christian Ott is with the Automation and Control Institute, Faculty of Electrical Engineering and Information Technology, TU Wien, 1040 Vienna, Austria christian.ott@tuwien.ac.at

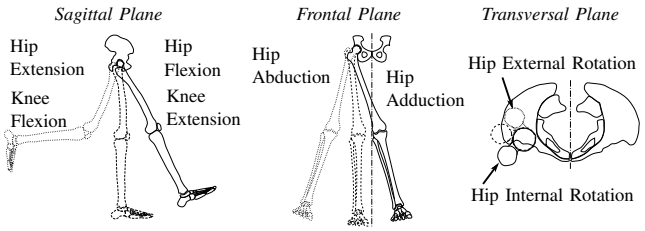

Fig. 2: Introduction to the human anatomy and the terminus of rotation.

the hip, knee and ankle. This complies with the standard robotic joint setup with six leg joints based on [18]. The ball-type hip joint enables motion in all three rotational degrees of freedom, while the knee, upper ankle, and subtalar joint have one degree of freedom. Accordingly, the main contributions of this paper are the review of oblique joint axes and the conclusion on effects/mechanisms for bipedal locomotion. The paper further contributes concepts using these mechanisms, which are introduced in a condensed form. The concepts can be seen as a guideline for the development of humanoid robots.

The paper is organized in the following concept: Sec. II is divided into each of the above-mentioned main joints. It introduces the human joint biomechanics and its mechanisms. The mechanisms are then elaborated in terms of their function for the human locomotion system and considered for the development of a humanoid robot kinematic. Sec. III proposes a guideline for the design and elaborates on the proposed mechanisms and reviews them for each type of locomotion. Finally, the results are summarized and potential applications as well as next steps are proposed.

II. Oblique Joint Axes

The following chapter introduces the main leg joints used for locomotion based on their order of importance. The biomechanic terminology is shown in Fig. 2 and introduces the most important terms which are used in the following chapter.

A. Knee Joint

The knee joint of the human is a complex rolling and sliding joint. The joint permits motion between the femur and the tibia bone. The leg bones are depicted in Fig. 3b The main motion occurs in the sagittal plane, and minor motion in the transversal plane. Strong ligaments are restricting the motion in the frontal plane. The patella bone interacts with the joint by sliding over the joint surface to attach the strong quadriceps femoris muscle at an advantageous lever position. The anterior and posterior cruciate ligaments restrict the translational movement in the anterior and posterior directions and guide the bones on the polycentric knee axis [19].

1) Polycentric knee mechanism: Fixing the knee axis to a static position does not represent its introduced functionality well. However, for robot development, a static axis reduces the complexity of the mechanical solution. The impact/ mechanism of a polycentric knee axis can be seen in the fully mechanical prosthetic *ReMotion Knee* (Equalize Health, CA, USA) [20]. A polycentric knee with a four-bar mechanism enables a passively stable stance phase under load due to an increased stable region in its singular position. The passive stability of the knee in the stance phase conforms to the rimless wheel/inverted pendulum type of motion in walking. However, the four-bar linkage increases the mechanical complexity for an elastic SLIP type of running. The knee axis in the transversal plane moves with the flexion of the knee and a reduced inclined position is present from $10° - 45°$ flexion [19], which is within the desired range of motion for the stance phase in running [21].

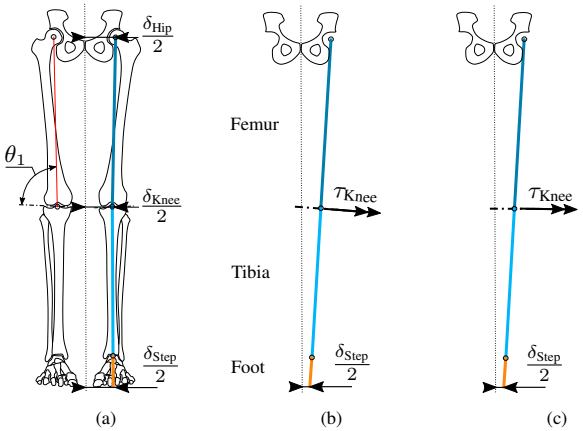

Fig. 3: Elaboration of the oblique knee axis (a) Biological axis of the knee $\theta_1 = 87°$; (b) orthogonal knee axis in the small step width setting; (c) oblique knee axis in the small step width setting results in a horizontal knee axis

2) Narrow step width mechanism: The literature reports an oblique mechanical knee axis of $\gamma = 3°$ adduction/valgus from the vertical axis of the hip center to the knee center, which is depicted by $\theta_1 = 90° - \gamma$ in Fig. 3a [17]. According to [22], the smaller the person, and the wider the hip width δ_{Hip}, the greater the adduction angle γ.

γ can be explained with the biological values for the step width δ_{Step}, and the hip width δ_{Hip}. A narrow step width aids human balance by lowering the medio-lateral ground reaction force (GRF) [23]. This is beneficial for movement, as the balancing load on the hip abductors decreases [24], [25]. The literature reports step widths of $5\,\text{cm} < \delta_{\text{Step}} < 13\,\text{cm}$ [26] for walking and $\delta_{\text{Step}} = 2.4\,\text{cm}$ for running [23]. An average human with a height of $170\,\text{cm}$, a leg length of $\delta_{\text{Leg}} = 90.1\,\text{cm}$ has an interhip width (between the hip center) of $\delta_{\text{Hip}} = 16.7\,\text{cm}$ [27], [28].

A knee axis that is aligned with the ground instead of being perpendicular to the femur or tibia as shown in Fig. 3b, explains the values for the adduction angle θ_1 in Fig. 3. With the rotated axis, the knee torque $\tau_{\text{Knee,flexion}}$ fully acts in the sagittal plane. Without the oblique knee axis, the knee torque is about $\eta_{\tau_{\text{Knee,flexion}}} = 1\,\%$ higher based on the following geometric equation:

$$\eta_{\tau_{\text{Knee,flexion}}} = \frac{1}{\cos(\gamma)}. \tag{1}$$

For the average human mentioned above with $\gamma = 3°$, a fully sagittal plane motion occurs at a step width of

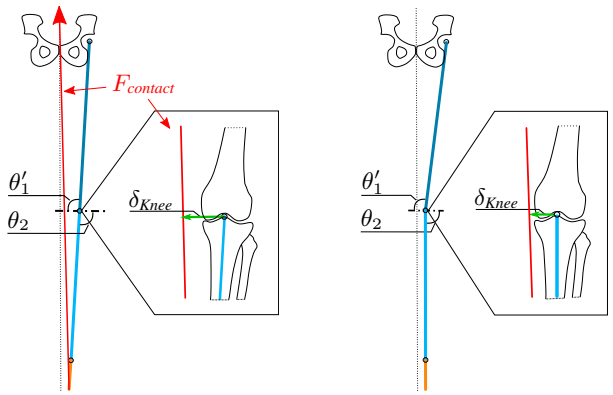

(a) (b)

Fig. 4: The oblique knee-tibia axis: (a) θ_1' and θ_2 are equal, this results in a larger δ_{Knee} between the solid-red F_{contact} (GRF) and the joint center compared to (b); and (b) θ_2 is $90°$ and θ_1' adapts to the desired step width. Based on (4) the constraint forces decrease.

$\delta_{\text{Step}} = 7.3\,\text{cm}$ based on (2), which complies with the range for walking.

$$\delta_{\text{Step}} = \delta_{\text{Hip}} - \sin(\gamma)\delta_{\text{Leg}}. \tag{2}$$

An oblique knee axis of $\gamma = 9.1°$ achieves a fully sagittal plane movement for running ($\delta_{\text{Step}} = 2.4\,\text{cm}$) calculated as:

$$\gamma = \arcsin(\frac{\delta_{\text{Hip}} - \delta_{\text{Step}}}{\delta_{\text{Leg}}}). \tag{3}$$

The mechanism of the oblique axis aligns the knee joint to an advantageous rotation plane when a reduced step width is used as depicted in Fig. 3c. We highly encourage to reduce the step width for a bipedal robot concept due to less frontal plane torque acting on the center of mass during movement. If the step width is reduced, we further encourage to introduce the oblique knee axis as well. It depends on the main task for the robot, how narrow the step width and thus how oblique the axis should be. The higher the running priority, the more oblique the knee axis can be.

3) Constraint torque mechanism : In addition to the oblique axis of the femur in Fig. 3a, the knee-tibia axis can also be inclined by θ_2 as depicted in Fig. 4b. A similar approach is used in orthopedics with insoles and wedges to shift the knee center towards the ground reaction force (GRF) vector [29]. This obliquity helps to reduce the medio-lateral constraint torque $\tau_{\text{Knee,constraint}}$. If applied, the angle between the femur and the knee axis should be increased to maintain the chosen step width.

This will primarily reduce the bearing weight $m_{bearing}$, which scales by an exponent of $m_{bearing} \approx \tau^{3/2}_{\text{Knee,constraint}}$ [30]. To show this effect, we calculate $\tau_{\text{Knee,constraint}}$ as,

$$\tau_{Knee,constraint} = \delta_{\text{Knee}} F_{\text{contact}}. \tag{4}$$

The oblique tibia setup results in $\delta_{\text{Knee}} = \delta_{\text{Step}}$ and reduces the constraint torque by $\eta_{\tau_{\text{Knee,constraint}}} = 25\,\%$ based on:

$$\eta_{\tau_{\text{Knee,constraint}}} = \frac{\delta_{\text{Step}}}{\text{mean}(\delta_{\text{Hip}}, \delta_{\text{Step}})}. \tag{5}$$

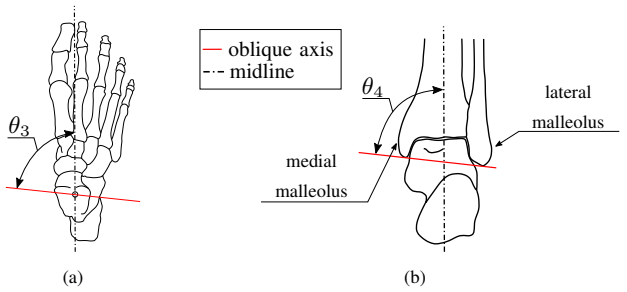

(a) (b)

Fig. 5: Upper ankle biological axis in the (a) transversal plane $\theta_3 = 84°$ and (b) frontal plane $\theta_4 = 80°$

4) Summary: In summary, the knee axis is oblique to align more closely with the horizontal axis at a narrow step width, which results in a higher portion of the torque being delivered to the mainly active sagittal plane of the robot. To reduce the constraint forces, the lower leg can be aligned with the GRF vector by rotating the tibia towards the sagittal plane. The polycentric knee axis is an additional mechanism which is valuable for the inverted-pendulum typed walking template.

B. Upper ankle joint

The talocrural or upper ankle joint is a hinge joint. The tibia and fibula are setting up a mortoise structure with the talus bone fitting between the two malleoli, as depicted in Fig. 5b. The literature reports multiple options for the oblique axis which diverge from the world frame axis [31], [32]. The main motion occurs in the sagittal plane. Fig. 5 shows the talocrural joint axis for the human kinematic. The axis rotates by $\theta_3 = 84°$ in the transversal and $\theta_4 = 80°$ in the frontal plane against their vertical axis [33]. The foot joints' obliquities are spanned over multiple joints, with mechanisms of the foot joints depending of each other, as elaborated in more detail in [9], [34].

1) Advanced foot mechanism: The upper ankle, subtalar (lower ankle), and transverse tarsal joint enable the supination/pronation motion of the foot. Supination and pronation is a coupled motion in the frontal, sagittal, and transversal plane. This motion of the foot complex has a strong effect on the center of pressure path in the human foot and is key to the mechanisms introduced in [9]. The foot joints guide the gait line/ center of pressure (COP) on the butterfly shaped path (regarding both feet), which uses the different stiffness of the lateral and medial compartments (arches) in the human foot (see Fig. 6). The medial elasticity is sometimes referred to as the windlass effect, as the plantar-aponeurosis (elastic tissue below the arch) stores the elastic energy and returns it at push off [35]. The windlass effect (longitudinal and transverse arch) can store up to $17\,\%$ of the energy from a running human at $4.5\,\text{m/s}$ [36]. The literature further reports that the ankle-foot complex (achilles tendon and arches) stores $52\,\%$ of the energy. The motion in the transversal plane plays a major role in these mechanisms, which are further elaborated in [9].

Resolving the question of an oblique axis in the upper

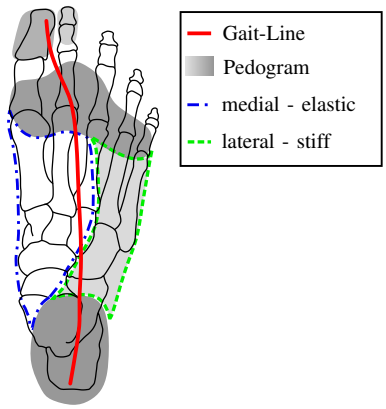

Fig. 6: Human foot gait line shown as the red path, the pedogram (pressure map) as a shade of gray, and the medial and lateral compartments; The gait line shows the single foot center of pressure path using the elastic structure in the medial compartment. Modified from [37]

ankle is closely related to the oblique axes of all the foot joints. This topic is out of this paper's scope, which comprises the six standard leg joints. Authors in [11], [12], [35] added additional foot joints to research the topics of the windlass effect and a transverse-tarsal/ Chopart joint.

2) Summary: It can be summarized that the decision for or against an oblique axis should be based on the desired complexity of the foot. Having two oblique foot joints and a non-elastic foot would increase the complexity of a humanoid without a large gain. However, structural elasticity may create a demand for a passive COP path generation. Additionally, in forefoot running, the joint should be aligned to the main active motion plane (horizontal axis) to be able to store more of the kinetic energy in the stance phase and to decrease the net work.

C. Subtalar joint

The subtalar joint (lower ankle) is set up between the talus and the calcaneus bone in the human foot. The bones are depicted in Fig. 7b. It is a typical hinge joint, which is necessarily held in place by ligaments and bone shapes. The main motion occurs in the frontal plane for lateral movements, which makes the joint important for adjusting the COP path and any kinematic which applies an advanced foot design or aims for any activity other than straight running (e.g. uneven ground, curves). Based on [38] the subtalar joint axis rotates by $\theta_5 = 23°$ in the transversal plane and $\theta_6 = 42°$ in the sagittal plane, also shown in Fig. 7b. The oblique axis has many advantages for walking and running locomotion. The inclined position can balance the COP and input a rotational impulse at push-off for curve running. In particular, the obliquity in the sagittal plane enables some easy-to-implement mechanisms.

1) Rocker gait mechanism: A walking dependent mechanism when using the rocker typed gait [39] is depicted in Fig. 8. At heel strike, the subtalar joint axis points upwards with a small angle between the GRF vector in the vertical direction. This transfers the high loads towards the proximal joints, which are mainly active in the sagittal plane. The heel

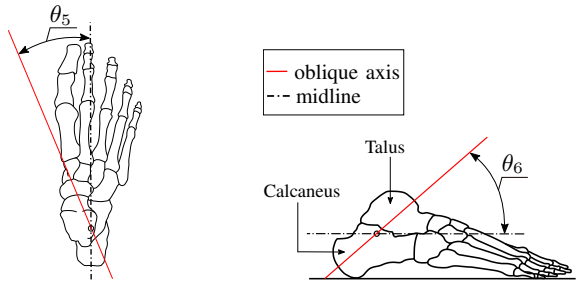

Fig. 7: Oblique subtalar axis in (a) transversal plane $\theta_5 = 16°$ and (b) sagittal plane $\theta_6 = 42°$

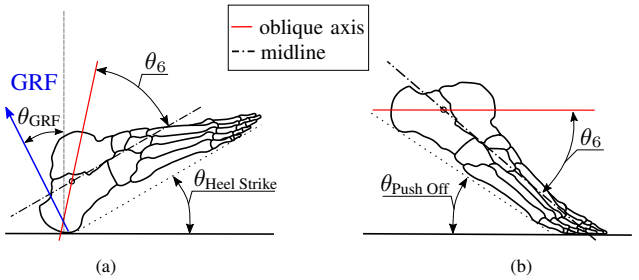

Fig. 8: Oblique subtalar axis at (a) heel strike (heel rocker) with $\theta_{\text{Heel Strike}} = 30°$ and $\theta_{\text{GRF}} = 42°$ [40], [41] and (b) push-off (forefoot rocker) with $\theta_{\text{Push Off}} = 48°$

enables a point-like contact shape while rotating the body over the heel rocker. Thus, the foot can place itself flat on the ground and set up a polygonal contact shape. In addition to this, the subtalar joint is able to adapt to inclinations by rotating around the axis. At lift-off, the foot has contact at the forefoot and the subtalar axis aligns nearly horizontal, which makes it possible to exert a high rotational torque in the frontal plane for lateral movements as depicted in Fig. 8b. The effect of an oblique subtalar axis was evaluated by [10]. The author conducts that the subtalar joint helps to reduce the error term for turning directions in a humanoid movement. In his case, the proposed obliquity of the sagittal plane performed close to the biological solution.

In case of the heel strike setup in Fig. 8a, the GRF is only partially supported by the subtalar joint actuator since the axis of rotation is rotated towards the GRF vector. The resulting lower reaction torque allows to use a smaller actuator for the subtalar joint. If the foot is placed slightly medial or lateral to the joint, the resulting impact torque on the oblique axis compares to the one on the perpendicular axis by a factor of $\eta_{\tau_{\text{impact}}} = 88.5\,\%$ as calculated as,

$$\eta_{\tau_{\text{impact}}} = \frac{\cos(\theta_6 + \theta_{\text{Heel Strike}} - \theta_{\text{GRF}})}{\cos(\theta_{\text{Heel Strike}} - \theta_{\text{GRF}})}. \tag{6}$$

Furthermore, the oblique joint has an increased ability to rotate the foot in the desired movement direction. In case of a heel strike angle of about $\theta_{\text{Heel Strike}} = 30°$ [40] the oblique axis can input a transversal torque $\eta_{\tau_{\text{transversal}}} = 90.2\,\%$ more efficiently using:

$$\eta_{\tau_{\text{transversal}}} = \frac{\sin(\theta_6 + \theta_{\text{Heel Strike}})}{\sin(\theta_{\text{Heel Strike}})}. \tag{7}$$

In stance phase, as seen in Fig. 7b, the oblique axis is used to correct the COP to balance the robot. In this case, the perpendicular axis is advantageous, as the oblique axis also input a torque into the transversal plane, which the hip needs to counteract.

Taking the configuration of Fig. 8b, a lateral push with the non-oblique subtalar joint will result in a $\eta_{\tau_{\text{frontal}}} = 34.5\,\%$ higher torque based on (8).

$$\eta_{\tau_{\text{frontal}}} = \frac{1}{\cos(\theta_6)}. \tag{8}$$

2) Summary: A humanoid robot, which aims for versatility with lateral movements, should make use of a sagittal plane deviation. The transversal obliquity should be reserved for advanced foot designs as introduced in Sec. II-B.1.

D. Hip Joint

The ball-and-socket type hip joint enables free rotational motion in all directions and thus does not have an oblique joint axis. However, it still has preferred motion directions based on the muscular system, with a large range of motions in the sagittal plane. The hip joint is set up between the pelvis and the femur bone. The joint is heavily surrounded by ligaments to hold the joint in its socket. The femur bone has an advantageous geometry/ lever arm for generating torques in the frontal plane (see Fig. 9 - Greater Trochanter), which are needed to resist the gravitational force of the body in the single support phase.

In human locomotion, the peak torque can be found in the frontal plane at single support stance time, while the largest impulse is found in the sagittal plane with the peak in the initial swing phase (40 % to 60 %) as shown in Fig. 10 [41]. The hip joint creates large accelerations in the early swing phase of running to propel the leg forwards and upwards, which is, after the ankle push off, the second largest contribution of propulsive power of the muscular skeleton system [42]. This peak power occurs prominently in robots without mechanisms which decrease the inertia of the swing or make use of joint couplings to distribute the demand.

1) Shared load mechanism: In humanoid robots, ball joints are set up by three serial rotational joints. The order has an impact and most robot hips use a Yaw-Roll-Pitch configuration based on [18], which are perpendicular to each other and aligned to the world coordinate system as depicted in Fig. 9 (I). Regarding joint efficiency, it is useful to rotate the joint axes out of the world coordinate system like the ARMAR IV and LOLA robots or other authors [13], [43] did to resolve singularities and to distribute the load over the actuators to avoid high peak loads in one actuator (e.g., in hip flexion or hip abduction) [14], [15].

The configuration in Fig. 9 (II) distributes peak torques based on the following mechanism. There is a rotation with the angle θ_{trans}, where the maximum peak torque of $\tau_2(\text{t})$ and $\tau_3(\text{t})$ is smaller than the maximum peak torque in the world frame aligned setup as described in (11). The rotated

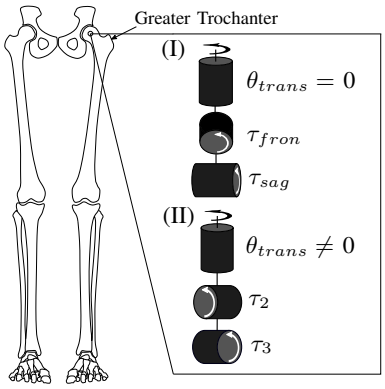

Fig. 9: Two different hip joint setups: (I) with an aligned axis to the world coordinate system and (II) θ_{trans} rotated towards the world coordinate system

torques $\tau_2(\text{t})$ and $\tau_3(\text{t})$ are calculated as

$$\tau_2(\text{t}) = \cos(\theta_{\text{trans}})\tau_{\text{sag}}(\text{t}) + \sin(\theta_{\text{trans}})\tau_{\text{fron}}(\text{t}), \tag{9}$$

$$\tau_3(\text{t}) = -\sin(\theta_{\text{trans}})\tau_{\text{sag}}(\text{t}) + \cos(\theta_{\text{trans}})\tau_{\text{fron}}(\text{t}). \tag{10}$$

As a result, the maximum torque becomes smaller as

$$\max(|\tau_2(\text{t})|, |\tau_3(\text{t})|) < \max(|\tau_{\text{fron}}(\text{t})|, |\tau_{\text{sag}}(\text{t})|). \tag{11}$$

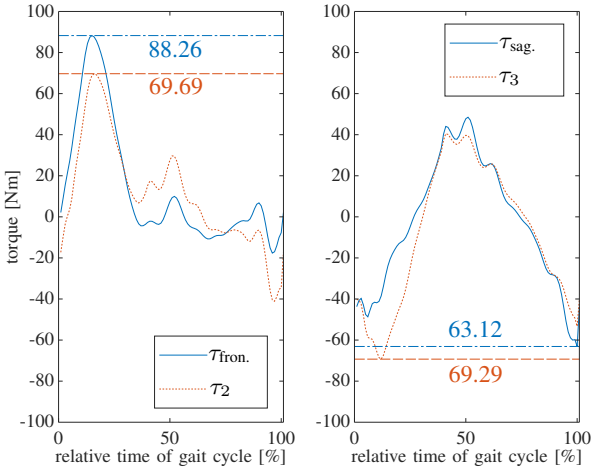

Fig. 10: Hip joint τ for a human running at 2.5 m/s [41]. The acting planes of τ are introduced in Fig. 9 for a world frame aligned- and a rotated setup by $\theta_{\text{trans}} = 26°$

In a robot design, the maximum torque an actuator has to output scales with its mass [30]. Furthermore, peak torque scales with electric motor losses.

We can show this effect with the dataset from [41]. We have used a rotation angle of $\theta_{\text{trans}} = 26°$ and applied (9)-(10). As visible in Fig. 10 the maximum torque in both actuators is reduced by 21.1 % from 88.3 Nm to 69.7 Nm.

2) Summary: In conclusion, a transversal rotation of the hip joint complex distributes the required hip torque between the two motors and decreases the torque and velocity peaks. This results in a lighter motor setup, which scales with the maximum demanded torque. However, it should be noted

that a rotated joint setup increases the complexity for the implementation of kinematic couplings and robot control.

III. A Guideline

In the previous sections, the oblique joints for walking and running were introduced. The main findings show that using an oblique joint axis approach can reduce the mechanical joint requirements of a humanoid robot. While the template models for the locomotion of walking and running differ, so does the applicability of these mechanisms. Especially due to the fact that the relationship between potential- and kinetic energy in walking is out of phase, while in running it is in phase [21].

A. Walking

Thus, for walking, a polycentric four-bar knee axis forces the leg on the inverted pendulum center of mass trajectory while being passively stable and enhancing the leg swing such that the foot swings forward into a stable ground position for a new touchdown. An oblique hip design, like the one of the ARMAR IV robot, should be considered and set up for the specific needs of the desired robot [14].

An advanced foot design that forces the COP on a desired trajectory in an elastic field can enable an energy storage of about $17\,\%$ as introduced in Sec. II-B.1. The rocker-typed walking template, which makes use of the rotational impulse, is mainly reserved for a walking- or slow running robot. With the three rockers: heel, ankle, and forefoot, the robot could use the mechanisms of the oblique subtalar joint axis by having a reduced load at heel strike and an advantageous joint axis for lateral movements in the pre-swing phase.

B. Running

The spring-mass template model for running desires the main motion in the active movement direction, which is the sagittal plane. Thus, the oblique joint axis of the knee, which rotates the foot as the endeffector to a narrower step width, helps to reduce medio-lateral external forces, which then decreases the total amount of work needed to resist these forces. Additionally, it reduces the amount of negative work in the hip, which is needed to resist the applied forces in the frontal plane due to a misaligned motion axis in movement direction and increases the amount of sagittal plane work for the same motor setup.

For running, a highly actuated sagittal plane is desirable, and using a forefoot running type enables the ankle joint to act as an additional spring. Here, the focus should be on setting a desired step width and adjusting the joint axis horizontally. However, for advanced running with direction changes, the subtalar joint takes on a crucial role by being able to input torque on a horizontal axis in the frontal plane, which generates a lateral rotational impulse prior to push-off. Especially in running, oblique axes need to be carefully considered and other biologically inspired mechanisms like multi-articulation and joint elasticity can have a higher impact.

IV. Conclusions

The review of oblique joint axes in the human musculoskeletal system revealed some significant mechanisms for humanoid kinematics that have yet to be applied to the field of humanoid robotics. Based on simple calculations, it can be shown that oblique axes in a humanoid robot can reduce the actuator torque requirements, the bearing load of the constraint torques, and thus the overall mass due to lighter actuators and bearings.

For further improvements, the advanced foot design from Sec. II-B.1 should be elaborated in more detail, to make use of the above mentioned $17\,\%$ energy return. The verification of the mechanisms in a humanoid robot setup will be conducted in the future, based on whole-body simulations. This paper should act as a guideline and toolbox for further humanoid robot developments by giving initial ideas of how to enhance a humanoid robot's kinematic by the inclination of the joint axes.

Acknowledgment

The authors are grateful to Jinoh Lee for his valuable input on the structure of this work.

References

[1] T. McGeer, "Passive Dynamic Walking," *The International Journal of Robotics Research*, vol. 9, no. 2, pp. 62–82, Apr. 1990.

[2] S. Kajita, F. Kanehiro, K. Kaneko, K. Yokoi, and H. Hirukawa, "The 3D linear inverted pendulum mode: A simple modeling for a biped walking pattern generation," in *Proceedings 2001 IEEE/RSJ International Conference on Intelligent Robots and Systems. Expanding the Societal Role of Robotics in the the Next Millennium (Cat. No.01CH37180)*, vol. 1, 2001, pp. 239–246.

[3] R. Blickhan, "The spring-mass model for running and hopping," *J Biomech*, vol. 22, no. 11-12, pp. 1217–1227, 1989.

[4] H. Geyer, A. Seyfarth, and R. Blickhan, "Compliant leg behaviour explains basic dynamics of walking and running," *Proceedings of the Royal Society B: Biological Sciences*, vol. 273, no. 1603, pp. 2861–2867, 2006.

[5] P. M. Wensing and D. E. Orin, "High-speed humanoid running through control with a 3D-SLIP model," in *2013 IEEE/RSJ International Conference on Intelligent Robots and Systems*, Nov. 2013, pp. 5134–5140.

[6] M. Hutter, C. D. Remy, M. A. Höpflinger, and R. Siegwart, "SLIP running with an articulated robotic leg," in *2010 IEEE/RSJ International Conference on Intelligent Robots and Systems*, Oct. 2010, pp. 4934–4939.

[7] D. M. Bramble and D. E. Lieberman, "Endurance running and the evolution of Homo," *Nature*, vol. 432, no. 7015, pp. 345–352, Nov. 2004.

[8] N. B. Holowka and D. E. Lieberman, "Rethinking the evolution of the human foot: Insights from experimental research," *Journal of Experimental Biology*, vol. 221, no. 17, p. jeb174425, Sep. 2018.

[9] C. W. Chan and A. Rudins, "Foot Biomechanics During Walking and Running," *Mayo Clinic Proceedings*, vol. 69, no. 5, pp. 448–461, May 1994.

[10] C. Lee, "Study of the human foot for the design of an anthropomorphic robot foot," *Thesis*, 2008.

[11] T. Kawakami and K. Hosoda, "Bipedal walking with oblique mid-foot joint in foot," in *2015 IEEE International Conference on Robotics and Biomimetics (ROBIO)*, Dec. 2015, pp. 535–540.

[12] S. Davis and D. G. Caldwell, "The design of an anthropomorphic dexterous humanoid foot," in *2010 IEEE/RSJ International Conference on Intelligent Robots and Systems*, Oct. 2010, pp. 2200–2205.

[13] R. W. Ellenberg, R. Vallett, R. J. Gross, B. Nutt, and P. Y. Oh, "Development of the skewed rotation plane (SRP) waist joint for humanoid robots," in *2013 IEEE Conference on Technologies for Practical Robot Applications (TePRA)*, Apr. 2013, pp. 1–6.

[14] T. Asfour, J. Schill, H. Peters, C. Klas, J. Bucker, C. Sander, S. Schulz, A. Kargov, T. Werner, and V. Bartenbach, "ARMAR-4: A 63 DOF torque controlled humanoid robot," in *2013 13th IEEE-RAS International Conference on Humanoid Robots (Humanoids)*, Oct. 2013, pp. 390–396.

[15] S. Lohmeier, T. Buschmann, and H. Ulbrich, "Humanoid robot LOLA," in *2009 IEEE International Conference on Robotics and Automation*, May 2009, pp. 775–780.

[16] Y. Asano, T. Kozuki, S. Ookubo, M. Kawamura, S. Nakashima, T. Katayama, I. Yanokura, T. Hirose, K. Kawaharazuka, S. Makino, Y. Kakiuchi, K. Okada, and M. Inaba, "Human mimetic musculoskeletal humanoid Kengoro toward real world physically interactive actions," in *2016 IEEE-RAS 16th International Conference on Humanoid Robots (Humanoids)*, Nov. 2016, pp. 876–883.

[17] J. J. Cherian, B. H. Kapadia, S. Banerjee, J. J. Jauregui, K. Issa, and M. A. Mont, "Mechanical, Anatomical, and Kinematic Axis in TKA: Concepts and Practical Applications," *Curr Rev Musculoskelet Med*, vol. 7, no. 2, pp. 89–95, Jun. 2014.

[18] J. B. Saunders, V. T. Inman, and H. D. Eberhart, "The major determinants in normal and pathological gait," *J Bone Joint Surg Am*, vol. 35-A, no. 3, pp. 543–558, Jul. 1953.

[19] M. a. R. Freeman and V. Pinskerova, "The Movement of the Knee Studied by Magnetic Resonance Imaging," *Clinical Orthopaedics and Related Research®*, vol. 410, pp. 35–43, May 2003.

[20] S. R. Hamner, V. G. Narayan, and K. M. Donaldson, "Designing for Scale: Development of the ReMotion Knee for Global Emerging Markets," *Ann Biomed Eng*, vol. 41, no. 9, pp. 1851–1859, Sep. 2013.

[21] T. F. Novacheck, "The biomechanics of running," *Gait & Posture*, vol. 7, no. 1, pp. 77–95, Jan. 1998.

[22] I. Kapandji, L. Honoré, and R. D'Aubigne, *The Physiology of the Joints: Annotated Diagrams of the Mechanics of the Human Joints. The Trunk and the Vertebral Column, with 397 Original Diagrams by the Author*. Churchill Livingstone, 1974, no. vol. 3.

[23] I. S. McClay and P. R. Cavanagh, "Relationship between foot placement and mediolateral ground reaction forces during running," *Clinical Biomechanics*, vol. 9, no. 2, pp. 117–123, Mar. 1994.

[24] C. J. Arellano and R. Kram, "The effects of step width and arm swing on energetic cost and lateral balance during running," *Journal of Biomechanics*, vol. 44, no. 7, pp. 1291–1295, Apr. 2011.

[25] S. Kubinski, C. A. McQueen, K. A. Sittloh, and J. C. Dean, "Walking with wider steps increases stance phase gluteus medius activity." *Gait & posture*, 2015.

[26] M. Whittle, *Gait Analysis: An Introduction*. Elsevier Science, 2014.

[27] R. Drillis and R. Contini, "Body Segment Parameters." New York Univ., N. Y. Research Div., Tech. Rep. PB174945, 1966.

[28] M. Williams and H. R. Lissner, *Biomechanics of Human Motion*, 6th ed. Philadelphia: Saunders, 1962.

[29] T. Sasaki and K. Yasuda, "Clinical evaluation of the treatment of osteoarthritic knees using a newly designed wedged insole," *Clin Orthop Relat Res*, no. 221, pp. 181–187, Aug. 1987.

[30] M. Budinger, J. Liscouet, and J.-C. Mare, "Estimation models for the preliminary design of electromechanical actuators," *Proceedings of the Institution of Mechanical Engineers, Part G: Journal of Aerospace Engineering*, vol. 226, pp. 243–259, Mar. 2012.

[31] L. Claassen, P. Luedtke, D. Yao, S. Ettinger, K. Daniilidis, A. M. Nowakowski, M. Mueller-Gerbl, C. Stukenborg-Colsman, and C. Plaass, "The geometrical axis of the talocrural joint—Suggestions for a new measurement of the talocrural joint axis," *Foot and Ankle Surgery*, vol. 25, no. 3, pp. 371–377, Jun. 2019.

[32] C. L. Brockett and G. J. Chapman, "Biomechanics of the ankle," *Orthopaedics and Trauma*, vol. 30, no. 3, pp. 232–238, Jun. 2016.

[33] D. A. Neumann, *Kinesiology of the Musculoskeletal System: Foundations for Rehabilitation*, third edition. ed. Elsevier, 2017.

[34] J. Hertel, "Functional Anatomy, Pathomechanics, and Pathophysiology of Lateral Ankle Instability," *Journal of athletic training*, vol. 37, pp. 364–375, Jan. 2003.

[35] K. Narioka, T. Homma, and K. Hosoda, "Humanlike ankle-foot complex for a biped robot," in *2012 12th IEEE-RAS International Conference on Humanoid Robots (Humanoids 2012)*, Nov. 2012, pp. 15–20.

[36] R. F. Ker, M. B. Bennett, S. R. Bibby, R. C. Kester, and R. M. Alexander, "The spring in the arch of the human foot," *Nature*, vol. 325, no. 6100, pp. 147–149, Jan. 1987.

[37] V. Stein and B. Greitemann, Eds., *Rehabilitation in Orthopädie und Unfallchirurgie*. Berlin, Heidelberg: Springer Berlin Heidelberg, 2005.

[38] S. K. Sarrafian, "Biomechanics of the subtalar joint complex," *Clin Orthop Relat Res*, no. 290, pp. 17–26, May 1993.

[39] J. Perry, *Gait Analysis: Normal and Pathological Function*. SLACK, 1992.

[40] J. Heidenfelder, T. Sterzing, M. Bullmann, and T. L. Milani, "Heel strike angle and foot angular velocity in the sagittal plane during running in different shoe conditions," *J Foot Ankle Res*, vol. 1, no. S1, p. 16, Sep. 2008.

[41] R. K. Fukuchi, C. A. Fukuchi, and M. Duarte, "A public dataset of running biomechanics and the effects of running speed on lower extremity kinematics and kinetics," *PeerJ*, vol. 5, p. e3298, May 2017.

[42] D. Thompson, "Power analysis of gait," https://ouhsc.edu/bserdac/dthompso/web/gait/epow/pow1.htm, Mar. 2002.

[43] M. Zorjan and V. Hugel, "Generalized humanoid leg inverse kinematics to deal with singularities," in *2013 IEEE International Conference on Robotics and Automation*, May 2013, pp. 4791–4796.